

Intra-guild predation (IGP) can increase or decrease prey density depending on the strength of IGP

FENG-HSUN CHANG ^{1,3} AND BRADLEY J. CARDINALE^{1,2}

¹*School for Environment and Sustainability, University of Michigan, 440 Church Street, Ann Arbor, Michigan, USA*

²*Cooperative Institute for Great Lakes Research (CIGLR), School for Environment and Sustainability, University of Michigan, 440 Church Street, Ann Arbor, Michigan, USA*

Citation: Chang, F.-H., and B. J. Cardinale. 2020. Intra-guild predation (IGP) can increase or decrease prey density depending on the strength of IGP. *Ecology* 101(7):e03012. 10.1002/ecy.3012

Abstract. In consumer communities, intra-guild predation (IGP) is a commonly observed interaction that is widely believed to increase resource density. However, some recent theoretical work predicts that resource density should first decrease, and then increase as the strength of IGP increases. This occurs because weak to intermediate IGP increases the IG predator density more than it reduces the IG prey density, so that weak to intermediate IGP leads to the lowest resource density compared to weak or strong IGP. We test this prediction that basal resource density would first decrease and then increase as the strength of IGP increase. We used a well-studied system with two protozoa species engaged in IGP and three bacteria species as the basal resources. We experimentally manipulated the percentage of the IG prey population that was available to an IG predator as a proxy for IGP strength. We found that bacterial density first decreased (by ~25%) and then increased (by ~30%) as the strength of IGP increased. Using a modified version of a published IGP model, we were able to explain ~70% of the variation in protozoa and bacterial density. Agreement of the empirical results with model predictions suggests that IGP first increased the IG predator density by consuming a small proportion of the IG prey population, which in turn increased the summed consumer density and decreased the bacterial resource density. As IGP strength increased further, the IG predator became satiated by the IG prey, which then freed the bacterial resource from predation and thus increased bacterial density. Consequently, our work shows that IGP can indeed decrease or increase basal resource density depending on its strength. Consequently, the impacts of IGP on resource density is potentially more complex than previously thought.

Key words: Blepharisma; Colpidium; competition; intra-guild predation; microcosms; population dynamics; predation; protozoa.

INTRODUCTION

Resource partitioning in space or time has been proposed to be the primary mechanism that allows consumers to minimize competition for resources (Hutchinson 1957, 1961, MacArthur 1958, Schluter 1993). When consumer species partitioning their resource use, a consumer community tends to be more efficient in capturing resources and, in turn, reduces resource density to a lower level (Duffy and Harvilicz 2001, Finke and Snyder 2008). However, there are several types of interspecific interaction that can either enhance or counter act the positive effects of resource partitioning on resource capture (Sih et al. 1998). These complex interactions include predator–prey interaction modifications (Sih et al. 1998), predator–predator facilitation (Losey and Denno 1998, 1999) and intra-guild predation (IGP; Polis et al. 1989, Polis and Holt 1992). These more complex interactions also influence how

efficiently prey resources are captured and consumed by a consumer community (Sih et al. 1998), and need to be considered along with the effects of resource partitioning if we are to better understand what controls the consumption of prey resources.

Among the various types of complex interactions that characterize consumers, intra-guild predation (IGP) is one of the most widespread and important (Barnes et al. 2018). IGP occurs when one consumer species (the intra-guild, IG predator) feeds on another one (the intra-guild, IG prey) with which it also competes for shared basal resources (Polis et al. 1989, Polis and Holt 1992). It has been reported that more than half of consumer taxa engage in IGP across terrestrial and aquatic systems (Arim and Marquet 2004, Thompson et al. 2007), and that 50% or more of taxa engage in IGP in the majority of natural communities (Dunne et al. 2004). The prevalence and uniqueness of IGP in consumer communities make IGP important for understanding how consumer species and their interactions determine basal resource consumption.

When IGP occurs, most theoretical studies predict that resource density will increase because consumer

Manuscript received 16 April 2019; revised 1 January 2020; accepted 3 January 2020. Corresponding Editor: Evan L. Preisser.

³E-mail: fhchang@umich.edu

assemblages will become less efficient in consuming their basal resources. The majority of these theoretical studies are based on the classic IGP model developed by Holt and Polis (1997). The classic IGP model predicted that when IGP occurs, the consumer community would be less efficient in consuming basal resources because the IG prey, which should be the more efficient consumer, had a lower density due to both competition and consumption pressure (Holt and Polis 1997). The prediction that IGP will always increase resource density remains qualitatively the same in more complex models that include (1) nonlinear functional responses (Kuijper et al. 2003), (2) additional species other than IG prey, IG predator and basal resource (Hart 2002), (3) additional trophic supplement to IG prey or predator (Daugherty et al. 2007), or that (4) allow IG prey or predator to also prey on themselves (Rudolf 2007).

But empirical studies have not always born out the expected positive impacts of IGP on basal resource density. For example, in a meta-analysis, Rosenheim and Harmon (2006) showed that IGP had nonsignificant effects on basal resource density because more than half (17 out of 29) of the studies showed lower, while the others showed higher, basal resource density when IGP occurs. A subsequent meta-analysis found that basal resource density generally increases with IGP (Vance-Chalcraft et al. 2007); yet, 48% of studies reviewed also showed decreased density of basal resource when IGP occurs.

Why is it that empirical studies have proven heterogeneous, with some finding that IGP increases prey density, while others find that IGP decreases prey density? Several factors have been proposed to explain the heterogeneous impacts of IGP on basal resource density. For example, in ecosystems where exploitative competition is more important than IGP in governing the population dynamics of IG prey and predator, occurrence of IGP decreases basal resource density (Vance-Chalcraft et al. 2007). In addition to ecosystem types, some IG predator species' feeding behavior might induce trait-mediated effects on IG prey and thus increase basal resource density (Preisser et al. 2005). Recently, Chang et al. (2020) offered another potential explanation. Using a simple consumer–resource model, they showed how the strength of IGP, i.e., number of IG prey consumed by an IG predator per time, can control whether IGP has a positive or negative effect on basal resource density. Specifically, their model predicted that basal resource density is a concave-up function of the strength of IGP. When IGP is weak to intermediate in strength, the IG predator increases more than the decrease of IG prey, such that the summed consumer density increases. In turn, the basal resource is subjected to the highest predation pressure, and thus has the lowest density, when IGP is weak to intermediate. Given these results, Chang et al. (2020) suggested that variation in the strength of IGP among consumer assemblages might be a plausible explanation for why IGP sometimes has positive, and other times negative effects on basal resource density in empirical studies. However, this prediction has yet to be

tested with any real biological system. Indeed, no empirical study to our knowledge has explicitly investigated how the strength of IGP affects basal resource density.

In this study, we used a well-developed study system of protozoa consuming bacteria (Morin 1999) to run an experiment to test the prediction that basal resource density is a concave-up function of the strength of IGP, first decreasing as IGP grows from weak to intermediate strengths, and then increasing as IGP grows from moderate to strong. The study system was composed of an omnivorous protozoa (the IG predator) that consumed a strict bacterivore (the IG prey) with which they competed for a common bacterial consortium (the basal resources). Using this system, we experimentally manipulated the percentage of the IG prey population that were accessible to the IG predator in order to vary the strength of IGP.

Our paper is organized according to the sequence of our research: First, we ran an experiment in which we manipulated the strength of IGP in the aforementioned system to determine how this impacts the density of the basal resource. Subsequently, we fit data from the experiment to predictions of Chang et al.'s IGP model and realized that while the two qualitatively agreed, quantitative agreement was poor. Third, suspecting the poor agreement was due to the overly simplistic Type I functional response used in the model, we performed a second experiment to characterize the functional response of the consumers. Fourth, after confirming the consumers do, in fact, follow a Type II functional response, we modified the model accordingly. This resulted in both qualitative and quantitative agreement between empirical results and model predictions, which allowed us to then use the model as a tool to deduce the biological mechanism that likely caused resource density to be a concave-up function of the strength of IGP.

METHOD

Experiment 1 methods

For the experiment, we used a protozoa–bacteria system that has been used previously to study the stability of food webs (Lawler and Morin 1993), and to examine how IG prey and predators coexist (Morin 1999, Banerji and Morin 2014). We used this protozoa–bacteria system to manipulate the strength of IGP, which was accomplished by altering the proportion of the IG prey population that were available for consumption by the IG predator (hereafter, availability of IG prey). Manipulating the proportion of IG prey available for consumption is akin to altering the probability that an IG predator would find an IG prey. The probability of a predator finding a prey is one of the components of the classic IGP model that determines the number of prey consumed by a predator per unit of time, i.e., attack rate (Holt and Polis 1997). We then tested if bacteria (basal resource) density at steady state was a concave-up

function of the strength of IGP, first decreasing, then increasing as the strength of IGP increased.

The focal organisms in the experiment were three bacteria species (*Serratia marcescens*, *Bacillus cereus*, and *Bacillus subtilis*) that served as the basal resource prey and two protozoa, *Colpidium striatum* (IG prey and a strict bacterivore) and *Blepharisma americanum* (IG predator and an omnivore) that served as the consumers (Morin 1999, Banerji and Morin 2014). The two protozoa species are known to engage in IGP, but are not known to exhibit other feeding relationships like cannibalism (Morin 1999). The focal species were cultured in ~300-mL experimental bottles that were made from two 240-mL Qorpak glass bottles (Qorpack, Bridgeville, PA, USA) that had their bottoms cut off, and which were then glued together with a Bolt Cloth-Nitex mesh (of varying size) (Wildco, Buffalo, NY, USA) installed in between.

The experiment included six treatments representing 0%, 20%, 40%, 60%, 80%, and 100% of the IG prey population being made available to the IG predator (Fig. 1). To create the 0% IGP strength treatment, the mesh size of the installed Bolt Cloth-Nitex mesh was 10 μm, which was not permeable to both consumers so that no IG prey were available to the IG predator. The 100% IGP strength treatment was created by replacing the 10-μm mesh with a 250-μm mesh that was permeable to both the IG prey and the IG predator, such that 100% of the IG prey population was available to the IG predator. For the other four treatments, 20-μm mesh that was permeable to the IG prey but not the IG predator was installed in the experimental bottles. To reassert that the 20-μm mesh was indeed permeable to the IG prey but not the IG predator, we used a microscope to confirm that the IG prey could

pass through the 20-μm mesh without difficulty but the movement of the IG predator was constrained by the 20-μm mesh. Therefore, the IG prey and the even smaller bacteria should be homogeneously distributed in the entire experimental unit except in the 0% IGP treatment. The location of the 20-μm mesh was manipulated to divide the entire experimental bottle into two spaces, a feeding space in which the IG prey was available to the IG predator, and a refuge space where the IG prey was not available. The ratio of the feeding space relative to the entire experimental bottle represented the availability of IG prey to the IG predator, and thus, the strength of IGP. By installing the 20-μm mesh in different position of the glass bottle, we created 20%, 40%, 60%, 80% IGP strength treatments, each of which was replicated five times.

Media for culturing protozoa species in the bottles was created by dissolving 0.07 mg "protozoan pellets" (Carolina Biological Supply, Burlington, North Carolina, USA) in 1 L of sterile deionized water in a 1,400-mL flask, after which the three bacteria species were inoculated. Then 200 mL of the media, two wheat seeds (one on each side of the experimental unit), and the protozoan species were added to the ~300-mL experimental bottle. The experimental bottles with cultured protozoa were placed on the Thermo Scientific MaxQ 2000 Benchtop Orbital Shakers (Waltham, MA, USA) to keep the organisms suspended under 60 rounds per minute (rpm), and the shakers were placed inside a growth chamber where temperature was set to 20°C.

During the experiment, we monitored the density of the two protozoa species every other day for 4 weeks. To track protozoa density, 5 mL of media in total was subsampled from both side of experimental bottle to count

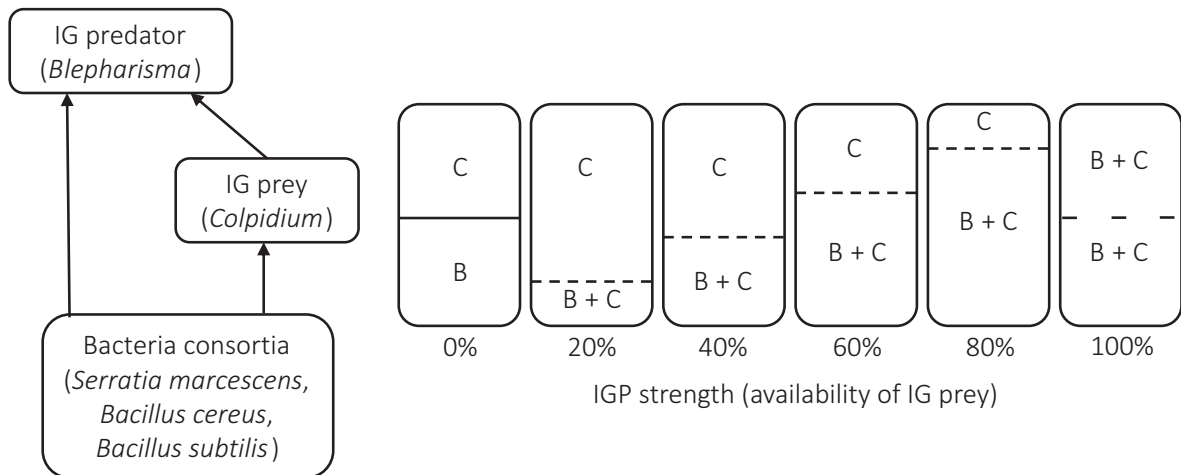


Fig. 1. Conceptual figure showing the simplified food web structure on the left and the experimental design of this study on the right. The squares on the right represent the six experimental treatments (0%, 20%, 40%, 60%, 80%, and 100% intra-guild predation [IGP] strength). The B and C in the rounded square are the initials of the IG predator (*Blepharisma*) and IG prey (*Colpidium*) species used in this study. The solid line in the first square from the left indicates that IG prey is not accessible to the IG predator (0% IGP). The dashed lines of the central four squares represent the 20-μm mesh that is permeable to IG prey but not IG predator. The location of the 20-μm mesh manipulates the percentage of IG prey that is accessible to IG predator: 20%, 40%, 60%, and 80% IGP strength. The long-dashed line in the rightmost square represents the 250-μm mesh that is permeable to both IG prey and predator so that 100% IGP is allowed.

the density of both protozoa species once every other day. After each subsampling, 5 mL fresh sterile media was supplied back to the experimental bottle to maintain the total volume. To count protozoan density, 100 μL of the subsampled media was used to count *Colpidium striatum* (IG prey) density and another 500 μL was used to count *Blepharisma americanum* (IG predator) density under $4\times$ dissecting microscope.

We used the monitoring data for protozoan densities to determine when the experimental units reached steady state with respect to protozoan population density. To assess steady state, we first calculated the mean density of both protozoa across five consecutive time points for each IGP treatment. We then gradually moved the five-point time window forward one time point at a time from hour 34 to hour 468, and divided the mean density of both protozoa in the present time window by that in the previous time window. The time window that showed the least change in protozoa density was defined as the steady state. Experimental systems reached steady state roughly 298 to 468 h after inoculation of protozoa (Appendix S1: Fig. S1).

We next measured bacteria densities at steady state to test the hypothesis that bacterial density first decreases and then increases with IGP strength. To quantify bacterial densities, we used an Attune Acoustic Focusing Cytometer (Thermo Scientific) to count bacteria of each replicate after the system reached steady state with respect to protozoa density. To prepare samples for the cytometer, all samples were passed through 20 μm mesh to remove large particles and to avoid clogging. In addition, if the cell density in a sample was higher than the recommended value by the Attune Acoustic Focusing Cytometer manual ($>10^6$ cells/mL), the sample would be rerun after diluted with Gibco™ PBS buffers (Thermo Scientific). Finally, we plotted the observed bacteria density vs. IGP strength and fitted a quadratic function to the data to statistically examine if the extreme values of bacteria density were located within the IGP strength range (0–100%) of our manipulation. If the coefficient associated with the quadratic term was significantly less than zero and the constant term was significantly greater than zero, we concluded that the bacteria density would first decrease and then increase with the increase of IGP strength. The fitting exercises were done by R 3.5.2 (R Core Team 2018).

Experiment 1 results

At steady state, we first fitted a quadratic function to the data to examine if the bacteria density exhibited a concave-up relationship vs. the strength of IGP. The quadratic function that best fitted to the data had a positive quadratic term (constant = 1; standard error = 0.14; $P < 0.01$; quadratic term = 1.42, standard error = 0.6, $P = 0.03$; $R^2 = 0.54$). The internal minimum of the quadratic function occurred at an IGP strength of 37% of the IG prey population being available to the IG predator (solid line of Fig. 2). As the strength of IGP increased from 0% to ~60%, the density of bacteria (basal resources) decreased

by roughly 25% ($P = 0.05$ for Tukey's Honest Significant Difference test comparing density between the 0–20% and 40–60% treatments). However, as the strength of IGP further increased to 80% and 100%, bacterial density increased by 36% relative to the 0% IGP treatment ($P = 0.02$ for Tukey's Honest Significant Difference test comparing density between 0–20% and 80–100% treatments; Fig. 2). Qualitatively, these experimental data match the theoretical prediction from Chang et al. (2020) that the strength of IGP first decreases, and then increases basal resource density.

Although the empirical data on bacteria density at steady state from experiment 1 qualitatively matched our a priori prediction, the empirical data (Fig. 2 solid dots) notably diverged from the model output of Chang et al. (2020), from which our predictions were derived (Fig. 2 long-dashed line). The difference between model predictions and empirical data (sum of square = 0.697) was greater than the total sums of squares of the data (0.365), which means the model prediction from Chang et al. (2020) was a poorer fit to the empirical data than the grand mean of the data. To improve the match between model predictions and empirical results, our first attempt was to parameterize Chang et al.'s with values from literature (Table 1). Unfortunately, parameterizing Chang et al.'s model with literature values further increase the difference between model predictions and empirical data (sum of square = 65.05; dotted line in Fig. 2). Because of the poor fit, we decided to pursue additional experimental work and model revisions that would achieve a better match of empirical data and theoretical predictions.

Experiment 2 methods

We suspected that the most likely reason why bacterial densities measured in Experiment 1 did not quantitatively match model predictions of Chang et al. (2020) was that the authors used an overly simplistic Type I functional response to model all consumption terms. In contrast to the simple Type I, some authors have suggested the consumption of bacteria by both *Colpidium* and *Blepharisma* may be better approximated by Type II functional response (Laybourn and Stewart 1975). To determine the type of functional response exhibited by the two protozoa species, we performed an additional experiment to quantify the functional response curve describing the consumption of IG prey by IG predator. This additional experiment was run in 60 mm (diameter) \times 15 mm (height) Fisherbrand Petri Dishes (Fisher Scientific, Hampton, NH, USA) with clear lids. We set up three replicate units for each of 10 treatments representing five levels of IG prey density with one IG predator individual, and the same five levels of IG prey density without IG predator. The five levels of IG prey density were created by mixing 2, 4, 6, 8, and 10 mL of media with *Colpidium* (IG prey) with 8, 6, 4, 2, and 0 mL of protozoa-free medium. The average density of IG prey of the five levels in the beginning was 4.11, 9.89, 15.11, 20, 29.78 individual/mL.

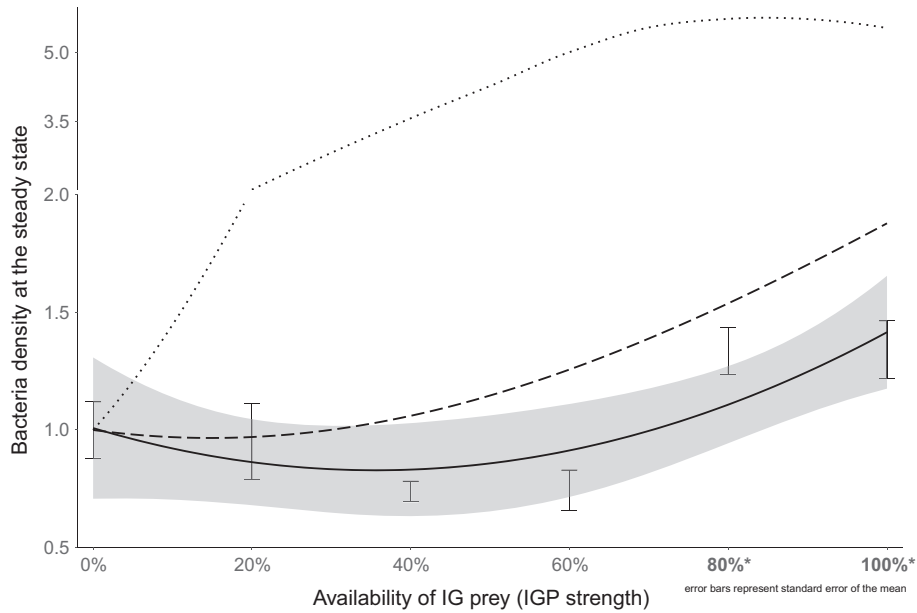


FIG. 2. Mean population density of bacteria when the experimental system reached steady state with respect to protozoa density (roughly hour 298 to 468) in different IGP strength treatments. The error bars represent the standard error of the mean. The 80% and 100% treatments have significantly higher bacteria density ($P < 0.01$). The three different lines represent (1) the quadratic function that best fits to the data (solid line with its standard error), (2) the predictions from the model of Chang et al. (2020) (long-dashed line), and (3) the model prediction when reparameterizing Chang et al.'s model (Type I model) with parameter values from literature. Note that both the long-dashed line and the dotted line are both from Chang et al.'s model but parameterized with different sets of values, which poorly fit the data (See the text in the section of “Experiment 1 results”).

The Petri dishes were then placed also on the Thermo Scientific MaxQ 2000 Benchtop Orbital Shakers rotating at 60 rpm in the same 20°C growth chamber. After 24 h, we recorded the density changes of IG prey in treatments with and without IG predator. The differences between the density changes in treatments with and without IG predator were the number of IG prey consumed per IG predator per day.

Experiment 2 results

By plotting the number of IG prey consumed per IG predator per day against the initial IG prey density, we found that a Type II saturating functional response (dashed line in Fig. 3a; $R^2 = 0.91$) was a better explanation of the intra-guild predation than Type I linear functional response ($P < 0.01$). From the Type II saturating function, the IGP attack rate and handling time were estimated to be 0.39 and 0.36, respectively. Given these results, we decided the next step was to modify all consumption terms in Chang et al. 2020 (Accepted) with a Type II functional response, and then parameterized the revised model with results of Experiment 2 (the IGP attack rate and handling time) or with values published in the literature.

A revised IGP model with type II functional response

Using the same general model structure as Chang et al. (2020), we used the following four equations to

describe the population dynamics of two basal resources as well as IG prey and predator

$$\frac{dR_1}{dt} = r_1 R_1 \left(1 - \frac{R_1}{K_1}\right) - \left[\frac{c_1 s R_1}{1 + h_1 c_1 s R_1 + h_1 c_1 (1-s) R_2} \right] Z_1 - \left[\frac{c_2 (1-s) R_1}{1 + h_2 c_2 (1-s) R_1 + h_2 c_2 s R_2 + h_3 c_3 \alpha Z_1} \right] Z_2 \quad (1)$$

$$\frac{dR_2}{dt} = r_2 R_2 \left(1 - \frac{R_2}{K_2}\right) - \left[\frac{c_1 (1-s) R_2}{1 + h_1 c_1 s R_1 + h_1 c_1 (1-s) R_2} \right] Z_1 - \left[\frac{c_2 s R_2}{1 + h_2 c_2 (1-s) R_1 + h_2 c_2 s R_2 + h_3 c_3 \alpha Z_1} \right] Z_2 \quad (2)$$

$$\frac{dZ_1}{dt} = \left[\frac{e_1 c_1 s R_1 + e_1 c_1 (1-s) R_2}{1 + h_1 c_1 s R_1 + h_1 c_1 (1-s) R_2} \right] Z_1 - \left[\frac{c_3 \alpha Z_1}{1 + h_2 c_2 (1-s) R_1 + h_2 c_2 s R_2 + h_3 c_3 \alpha Z_1} \right] Z_2 - m Z_1 \quad (3)$$

$$\frac{dZ_2}{dt} = \left[\frac{e_2 c_2 (1-s) R_1 + e_2 c_2 s R_2 + e_3 c_3 \alpha Z_1}{1 + h_2 c_2 (1-s) R_1 + h_2 c_2 s R_2 + h_3 c_3 \alpha Z_1} \right] Z_2 - m Z_2 \quad (4)$$

In accordance with Chang et al. (2020), the dynamics of bacteria species (R_1 and R_2), IG prey (Z_1) and

TABLE 1. Parameter values used for model with Type I functional response in Chang et al. (2019) and model with Type II functional response in this study.

Parameter	Value			Source for Type II model
	Chang et al.'s Type I model	Chang et al.'s Type I model (with literature values)	Type II model	
Bacteria per capita growth rate (r_i ; 1/d)	2.5	1.72	1.72	Ratkowsky et al. (1982), Fedrigo et al. (2011)
Bacteria carrying capacity (K_i ; individuals/mL)	50×10^5	8.14×10^5 †	8.14×10^5 †	empirically measured
Attack rate of <i>Colpidium</i> (IG prey) on bacteria (c_1 ; $1 \cdot d^{-1} \cdot \text{consumer}^{-1}$)	1	1.25	1.25	Laybourn and Stewart (1975)
Handling time of <i>Colpidium</i> (IG prey) on bacteria (h_1 ; $d \cdot \text{consumer}^{-1} \cdot \text{resource}^{-1}$)	N.A.	N.A.	0.08×10^5	Laybourn and Stewart (1975)
Assimilation efficiency from bacteria to <i>Colpidium</i> (IG prey) (e_1 ; %)	0.3	0.11	0.11	Laybourn and Stewart (1975)
Attack rate of <i>Blepharisma</i> (IG predator) on bacteria (c_2 ; $1 \cdot d^{-1} \cdot \text{consumer}^{-1}$)	0.7	1.25	1.25	same as <i>Colpidium</i> but see Appendix S2
Handling time of <i>Blepharisma</i> (IG predator) on bacteria (h_2 ; $d \cdot \text{consumer}^{-1} \cdot \text{resource}^{-1}$)	N.A.	N.A.	0.8×10^5 ‡	Laybourn and Stewart (1975), Fenchel (1980)
Assimilation efficiency from bacteria to <i>Blepharisma</i> (IG predator) (e_2 ; %)	0.3	0.11	0.11	same as <i>Colpidium</i> but see Appendix S2
IGP attack rate (c_3 ; $1 \cdot d^{-1} \cdot \text{consumer}^{-1}$)	1	0.39	0.39	empirically measured
IGP handling time (h_3 ; $\text{day} \cdot \text{consumer}^{-1} \cdot \text{resource}^{-1}$)	N.A.	N.A.	0.36	empirically measured
IGP assimilation efficiency (e_3 ; $\text{day} \cdot \text{consumer}^{-1} \cdot \text{resource}^{-1}$)	1	0.4	0.4	Fig. 3b
Degree of resource partitioning (s)	0.75	0.96	0.96	Fig. 3b
Density independent mortality (m)	1	0.1	0.1	empirically measured

†This bacterial density should be high enough for the IG predator to exhibit nonsignificantly different bacterial consumption rate among IGP treatments.

‡This value was estimated from the fact that the maximum food uptake rate (which should be the inverse of handling time) of *Colpidium* was 10 times higher than that of *Blepharisma* (Fenchel 1980).

predator (Z_2) were described by Eqs. 1–4, respectively. The two basal resources grew logistically with intrinsic growth rates r_1 and r_2 , as well as carrying capacities K_1 and K_2 . Both basal resources were consumed by IG prey (Z_1) and IG predator (Z_2) following a Type I functional response with attack rate (c_i), where $i = 1$ or 2 indicating IG prey or IG predator, respectively. Following Chang et al. (2020), the parameter s , ranging from 0.5 to 1, was designed to manipulate the degree of resource partitioning among IG prey and predator. When $s = 0.5$, both consumers become complete generalists consuming equally on both resources. When $s = 1$ the IG prey (Z_1) was a complete specialists consuming R_1 , and the predator (Z_2) was completely specialized on R_1 . The dynamics of IG prey (Z_1) and IG predator (Z_2) were described by Eqs. 3 and 4. Growth rate of IG prey and IG predator was determined by the consumption terms, which now followed a Type II functional response, multiplied the assimilation efficiency (e_i). In addition, the IG predator also consumed the IG prey, i.e., the intra-guild predation, following also a Type II functional response with the IGP attack rate (c_3), handling time (h_3), assimilation efficiency (e_3), and the parameter α describing the availability of IG prey to IG predator. The α is the strength

of IGP that is the focus of this study. Finally, both IG prey and predator had a density independent mortality (m_1 and m_2).

To generate predictions from the Type II model (Eqs. 1–4), we parameterized the model with values from experiment 2 (the IGP attack rate and handling time; Fig. 3a) and the published literature (Type II model column of Table 1), with exception of two parameters: the assimilation efficiency from IG prey to IG predator (e_3) and the degree of resource partitioning (s). We estimated the assimilation efficiency from IG prey to IG predator (e_3) and the degree of resource partitioning (s) by searching for the combination of two parameters that yielded the least difference between model predictions and empirical data. To estimate the difference between model predictions and empirical data, we first plotted the summed density of bacteria as well as the density of IG prey and predator at steady state against IGP strength (α), i.e., 0%, 20%, 40%, 60%, 80%, and 100% of IG prey available to IG predator. These empirical patterns were overlaid with predictions from the Type II model to calculate the residual sum of squares of the model predictions. Note that the model predictions were calculated from the long-term average (last

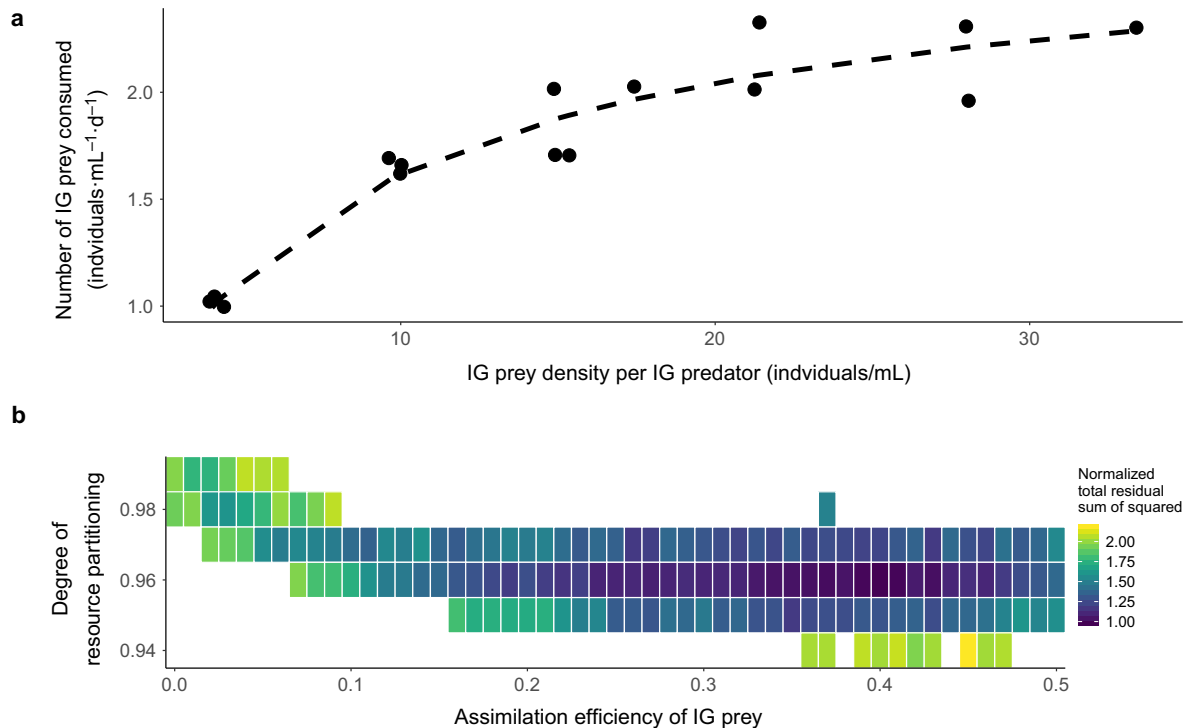


FIG. 3. (a) Type II functional response of intra-guild predation, i.e., number of IG prey consumed against IG prey vs. IG predator ratio. The two parameters describing the Type II functional response, IGP attack rate and handling time of *Blepharisma* (IG predator) on *Colpidium* (IG prey), are estimated to be 0.39 and 0.36, respectively. (b) The total residual sum of squares of the model with different combinations of the two unknown parameters, the degree of resource partitioning between IG prey and predator as well as the assimilation efficiency from IG prey to IG predator. At a given combination of the two parameter values, the normalized total residual sum of square of the model for bacteria, IG prey and predator density is calculated and represented by the color of the tile. White space represents the combination that the model results in higher normalized total residual sum of squared than just the average across intra-guild predation treatments (a null model). The model has the lowest total residual sum of square when the degree of resource partitioning is 0.96 and the assimilation efficiency is 40%.

2,000 time steps of the 10,000 simulated time steps) of two resources, Z_1 and Z_2 because the model appears to exhibit limit cycle behaviors (Appendix S1 and Appendix S1: Fig. S2). By doing this, we found the best parameter value combination of assimilation efficiency (e_3) and degree of resource partitioning (s) to be 40% and 96%, respectively (Fig. 3b). The model predictions were generated with the aid of Mathematica 11.1 (Wolfram Research 2017), and the difference between model predictions and empirical data was done by R 3.5.2 (R Core Team 2018).

The revised IGP model with a Type II functional response explained 67%, 68%, and 66% of the variance for summed bacterial density, as well as the density of the IG prey and the density of the IG predator at steady state in experiment 1, respectively (Fig. 4). The model with a Type II functional response more appropriately captured the threshold of bacteria density (40–60% availability of IG prey population to IG predator) beyond which bacteria density started to increase with the strength of IGP (Fig. 4a). For the IG prey density at steady state, the Type II model also predicted the monotonic decrease from 0% to 100% IGP strength (the solid

line in Fig. 4b) that was observed in the experiment (solid dots in Fig. 4b). Finally, for the IG predator density, the Type II model and the experimental data suggested that IGP strength actually increased and then leveled off (Fig. 4c). Given the improved match between empirical data and predictions from the Type II model, we can infer that the decrease and then increase of bacterial density at steady state (Figs. 2, 4a) resulted from the saturating Type II functional response of consumers involved in IGP (explained further in *Discussion*).

DISCUSSION

Our experimental results showed that, at the steady state, the density of basal prey resource (bacteria) was a concave-up function of intra-guild predation: first decreasing, and then increasing as the strength of IGP increased (Figs. 2, 4a). This finding supports the theoretical prediction from Chang et al. (2020) that intra-guild predation strength would first decrease and then increase the density of basal resource. This finding could help explain why some empirical studies have demonstrated negative effects of IGP on basal resource

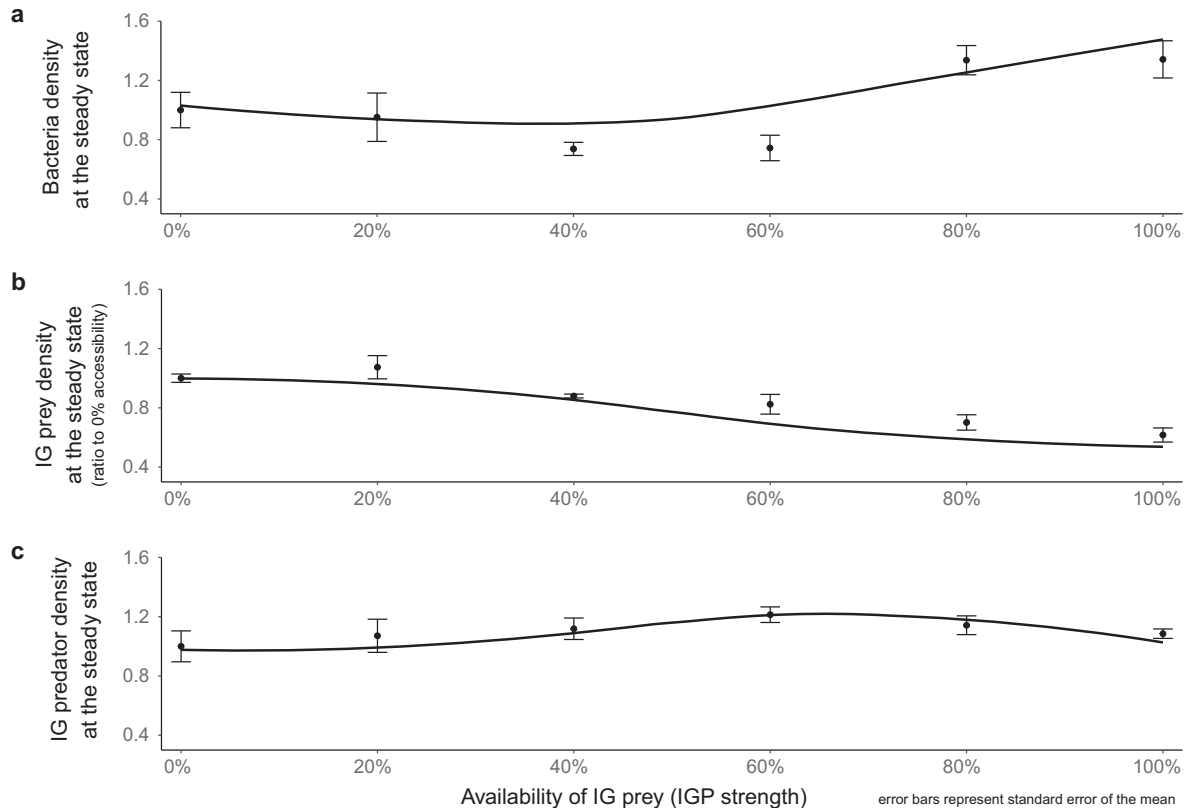


FIG. 4. Population density of (a) bacteria, (b) IG prey, and (c) IG predator when the experimental system reached steady state with respect to protozoa density (roughly hour 298 to 468) in different IGP strength treatments. The error bars represent the standard error of the mean. The solid lines represent the predictions from the model with Type II functional response (Type II model). The solid lines explain 66%, 68.08%, and 67.45% of the variance across the six IGP strength treatments (0–100%) for IG predator, IG prey, and bacteria density, respectively.

density, whereas others have shown the opposite (Vance-Chalcraft et al. 2007).

The observed population dynamics of bacteria, IG prey and predator were explained reasonably well (~70%) by an IGP model that was modified to have a Type II functional response (solid lines in Fig. 4). That model was partly parameterized with literature values and partly parameterized by our own experimental work. The Type II model helped identify potential biological mechanisms that might underlie the patterns observed in experiment 1. When the IGP strength increased from 0% to more moderate levels (e.g., 40–60%), the IG predator density increased due to moderate consumption of the IG prey. The summed consumer density was, therefore, higher such that bacteria density was suppressed to the lowest level. When the strength of IGP increased further, the IG predator started to be satiated by the IG prey such that the IG predator stopped consuming bacteria and the IG prey density reached the lowest level. Consequently, the lowest level of IG prey density and satiated IG predator resulted in the lowest bacterial consumption and thus highest bacterial resource density at equilibrium (Figs. 2, 4).

The fit of the Type II model to data from the experiment is a bit of a double-edged sword. On one hand, the model did appear to qualitatively capture the concave-up relationship between the strength of IGP and the density of the bacterial resources, which was our original prediction based on previous theoretical work. In addition, the model was a reasonable fit to this concave-up relationship, explaining approximately 70% of the variation in empirical data. On the other hand, the Type II model that we developed failed to mimic certain aspects of the temporal dynamics of the experiment. Indeed, population densities of the IG prey and predator reached a steady state over the time frame of the experiment (Appendix S1: Fig. S1), whereas the Type II model was characterized by limit cycles (Appendix S1: Fig. S2). While the mean values of the model matched those from the experiment, there clearly was a mismatch in temporal dynamics that suggests certain aspects of biology are still missing from model. We speculate that the most likely mismatch lies in the accuracy of the measures of bacterial growth rate and/or conversion efficiencies from bacteria to protozoa. A reduction in these parameter values could potentially dampen the limit cycles. Despite

clear limitations of the model, we feel that an imperfect quantitative description of the experimental system is better than none at all.

Though the assimilation efficiency from IG prey to IG predator has not been empirically measured, it is possible to infer a value using size spectrum theory (Kerr 1974, Sheldon et al. 1977). According to the size spectrum theory, an individual's consumption rate and volumetric search rate should scale with body size as a power law with scaling exponents of 0.75 and 0.80, respectively (Andersen and Beyer 2006). Given those scaling exponents and the predator-prey body size ratio in our study (Long and Morin 2005), the assimilation efficiency is predicted to be 41.7% (Andersen et al. 2009), which is similar to our fitted estimate (40%).

While the value for assimilation efficiency is consistent with other lines of evidence, we are somewhat skeptical of the value we obtained for resource partitioning between the IG prey and IG predator. Our model suggested there was a 96% separation in food items consumed by the IG predator and the IG prey. While the two species certainly exhibit resource partitioning, biologically, these two species are both filter feeders with relatively similar ciliary structures (Fenchel 1980). Because complete partitioning of bacterial resources seems unlikely, this particular parameter needs to be verified or refined with additional experiments.

In addition to the two fitted parameters (e_3 and s), attack rate (c_2) and assimilation efficiency (e_2) of *Blepharisma* on bacteria were set to be the same as that of *Colpidium*. We made this decision because both species were both filter feeders (Verni and Gualtieri 1997, Thurman et al. 2010) and they fed on the same food resources in our experiments although these two parameters may differ among the two species. However, altering the value of these two parameters did not appear to qualitatively change the match between model predictions and empirical results (Appendix S2). After altering the value of attack rate (c_2) and assimilation efficiency (e_2) we still found the density of basal resources first decrease and then increase with intra-guild predation. Consequently, the value of attack rate (c_2) and assimilation efficiency (e_2) of *Blepharisma* on bacteria can differ from that of *Colpidium* but such difference should not change our conclusions.

Our experiment suffers all the caveats that are typical of microcosm experiments (Briggs and Borer 2005). These caveats include small temporal and spatial scale, restricted environmental variability and species interactions, as well as lack of natural trophic structures. In addition, our experimental setup differs from the model, although we have done our best efforts to design and parameterize the model to match the empirical experiments. In the experiments, there were three bacteria species, but there were two resources in the theoretical model. We can only speculate how having the third resource in the theoretical model might influence the model agreement to our empirical work. One of our

speculations was that including the third resource only increased the degree of resource partitioning if the third resource was mainly consumed by IG prey or predator. Since the degree of resource partitioning was already estimated to be very high (96%), having the third resource might not influence the match between theoretical model and empirical results. On the other hand, addition of the third resource might decrease the degree of resource partitioning if the third resource was evenly consumed by IG prey and predator or the third resource might change the population density of IG prey or predator. In such scenario, the match between theoretical predictions and empirical results would be deteriorated. We can't discern the actual impacts of having the third resource before more research has been done. Nevertheless, we would point out that our goal in this study is not to extend results to real aquatic ecosystems. Rather, the point of a microcosm experiment like this one is to test a specific theoretical prediction in highly controlled environment. Now that we have done so, the next obvious step is to similarly test the prediction using observational studies or experiments in more natural systems.

To our knowledge, this is the first empirical study to explicitly investigate how the strength of intra-guild predation impacts basal resource density. Our finding that IGP can decrease or increase basal resource density depending on its strength runs counter to the conventional thinking that IGP always interferes the ability of consumers to control basal resources and, in turn, always increases basal resource density. Our study suggests that the impacts of IGP could be more complex than previously expected. Therefore, if we are to better understand what controls the consumption of basal resources, we may need to explicitly quantify the strength of intra-guild predation.

ACKNOWLEDGMENTS

We thank Peter Morin's research group for their kindly help on microcosm setup and consultant. We thank Inés Ibáñez and Casey Godwin for their valuable advice and feedback on the manuscript and Po-Ju Ke on the theoretical consultant. We especially thank Holly Moeller for her willingness to discuss with us regarding various aspects of the manuscript. Her comments ultimately strengthened the manuscript. This work is sponsored by the scholarship of government sponsorship for overseas study, Ministry of Education, Taiwan and Rackham One-Term Dissertation Fellowship, University of Michigan.

LITERATURE CITED

- Andersen, K. H., and J. E. Beyer. 2006. Asymptotic size determines species abundance in the marine size spectrum. *American Naturalist* 168:54–61.
- Andersen, K. H., J. E. Beyer, and P. Lundberg. 2009. Trophic and individual efficiencies of size-structured communities. *Proceedings of the Royal Society B* 276:109–114.
- Arim, M., and P. A. Marquet. 2004. Intraguild predation: a widespread interaction related to species biology. *Ecology Letters* 7:557–564.

- Banerji, A., and P. J. Morin. 2014. Trait-mediated apparent competition in an intraguild predator–prey system. *Oikos* 123:567–574.
- Barnes, A. D., M. Jochum, J. S. Lefcheck, N. Eisenhauer, C. Scherber, M. I. O'Connor, P. de Ruiter, and U. Brose. 2018. Energy flux: the link between multitrophic biodiversity and ecosystem functioning. *Trends in Ecology and Evolution* 33:186–197.
- Briggs, C. J., and E. T. Borer. 2005. Why short-term experiments may not allow long-term predictions about intraguild predation. *Ecological Applications* 15:1111–1117.
- Chang, F. H., P. J. Ke, and B. Cardinale. 2020. Weak intra-guild predation facilitates consumer coexistence but does not guarantee higher consumer density. *Ecological Modelling* 424. <https://doi.org/10.1016/j.ecolmodel.2020.109019>
- Daugherty, M. P., J. P. Harmon, and C. J. Briggs. 2007. Trophic supplements to intraguild predation. *Oikos* 116:662–677.
- Duffy, J. E., and A. M. Harvilicz. 2001. Species-specific impacts of grazing amphipods in an eelgrass-bed community. *Marine Ecology Progress Series* 223:201–211.
- Dunne, J., R. J. Williams, and N. D. Martinez. 2004. Network structure and robustness of marine food webs. *Marine Ecology Progress Series* 273:291–302.
- Fedrigo, G. V., E. M. Campoy, G. Di Venanzio, M. I. Colombo, and E. García Vescovi. 2011. *Serratia marcescens* is able to survive and proliferate in autophagic-like vacuoles inside non-phagocytic cells. *PLoS ONE* 6:e24054.
- Fenchel, T. 1980. Suspension feeding in ciliated protozoa: Feeding rates and their ecological significance. *Microbial Ecology* 6:13–25.
- Finke, D. L., and W. E. Snyder. 2008. Niche increases resource partitioning by diverse communities exploitation. *Science* 321:1488–1490.
- Hart, D. R. 2002. Intraguild predation, invertebrate predators, and trophic cascades in lake food webs. *Journal of Theoretical Biology* 218:111–128.
- Holt, R. D., and G. A. Polis. 1997. A theoretical framework for intraguild predation. *American Naturalist* 149:745–764.
- Hutchinson, G. E. 1957. Concluding remarks. *Cold Spring Harbor Symposia on Quantitative Biology* 22:415–427.
- Hutchinson, G. E. 1961. The paradox of the plankton. *American Naturalist* 95:137–145.
- Kerr, S. R. 1974. Theory of size distribution in ecological communities. *Journal of the Fisheries Research Board of Canada* 31:1859–1862.
- Kuijper, L. D. J., B. W. Kooi, C. Zonneveld, and S. A. L. M. Kooijman. 2003. Omnivory and food web dynamics. *Ecological Modelling* 163:19–32.
- Lawler, S. P., and P. J. Morin. 1993. Food web architecture and population dynamics in laboratory microcosms of protists. *American Naturalist* 141:675–686.
- Laybourn, J. E. M., and J. M. Stewart. 1975. Studies on consumption and growth in the ciliate *Colpidium campylum* Stokes. *Journal of Animal Ecology* 44:165–174.
- Long, Z. T., and P. J. Morin. 2005. Effects of organism size and community composition on ecosystem functioning. *Ecology Letters* 8:1271–1282.
- Losey, J. E., and R. F. Denno. 1998. Positive predator–predator interactions: enhanced predation rates and synergistic suppression of aphid populations. *Ecology* 79:2143–2152.
- Losey, J. E., and R. F. Denno. 1999. Factors facilitating synergistic predation: the central role of synchrony. *Ecological Applications* 9:378–386.
- MacArthur, R. H. 1958. Population ecology of some warblers of northeastern coniferous forests. *Ecology* 39:599–619.
- Morin, P. 1999. Productivity, intraguild predation, and population dynamics in experimental food webs. *Ecology* 80:752–760.
- Polis, G. A., and R. D. Holt. 1992. Intraguild predation: the dynamics of complex trophic interactions. *Trends in Ecology and Evolution* 7:151–154.
- Polis, G. A., C. A. Myers, and R. D. Holt. 1989. The ecology and evolution of intraguild predation: potential competitors that eat each other. *Annual Review of Ecology and Systematics* 20:297–330.
- Preisser, E. L., D. I. Bolnick, and M. F. Benard. 2005. Scared to death? The effects of intimidation and consumption in predator–prey interactions. *Ecology* 86:501–509.
- R Core and Team. 2018. R: a language and environment for statistical computing. R Project for Statistical Computing, Vienna, Austria. <https://www.r-project.org/>
- Ratkowsky, D. A., J. Olley, T. A. McMeekin, and A. Ball. 1982. Relationship between temperature and growth rate of bacterial cultures. *Journal of Bacteriology* 149:1–5.
- Rosenheim, J. A., and J. P. Harmon. 2006. The influence of intraguild predation on the suppression of a shared prey population: an empirical reassessment. Pages 1–20 in J. Broder and G. Boivin, editors. *Trophic and guild in biological interactions control*. Springer Netherlands, Dordrecht, The Netherlands.
- Rudolf, H. W. V. 2007. The interaction of cannibalism and omnivory: consequences for community dynamics. *Ecology* 88:2697–2705.
- Schluter, D. 1993. Adaptive radiation in sticklebacks: size, shape, and habitat use efficiency. *Ecology* 74:699–709.
- Sheldon, R. W., W. H. Sutcliffe Jr., and M. A. Paranjape. 1977. Structure of pelagic food chain and relationship between plankton and fish production. *Journal of the Fisheries Research Board of Canada* 34:2344–2353.
- Sih, A., G. Englund, and D. Wooster. 1998. Emergent impacts of multiple predators on prey. *Trends in Ecology and Evolution* 13:350–355.
- Thompson, R. M., M. Hemberg, B. M. Starzomski, and J. B. Shurin. 2007. Trophic levels and trophic tangles: the prevalence of omnivory in real food webs. *Ecology* 88:612–617.
- Thurman, J., J. D. Parry, P. J. Hill, and J. Laybourn-Parry. 2010. The filter-feeding ciliates *Colpidium striatum* and *Tetrahymena pyriformis* display selective feeding behaviours in the presence of mixed, equally-sized, bacterial prey. *Protist* 161:577–588.
- Vance-Chalcraft, H. D., J. A. Rosenheim, J. R. Vonesh, C. W. Osenberg, and A. Sih. 2007. The influence of intraguild predation on prey suppression and prey release: a meta analysis. *Ecology* 88:2689–2696.
- Verni, F., and P. Gualtieri. 1997. Feeding behaviour in ciliated protists. *Micron* 28:487–504.
- Wolfram Research. 2017. Mathematica, Version 11.2. Wolfram Research, Champaign, Illinois, USA.

SUPPORTING INFORMATION

Additional supporting information may be found in the online version of this article at <http://onlinelibrary.wiley.com/doi/10.1002/ecy.3012/supinfo>